AD-A276 690

SENSITIVITY ANALYSIS OF THE AVHRR INFRARED CIRRUS MODEL

Allan J. Bussey
Robert P. d'Entremont

19 July 1993

DTIC
ELECTE
FEB. 0.9 1994
S
B
D

Approved for Public Release; distribution unlimited

PHILLIPS LABORATORY
Directorate of Geophysics
AIR FORCE MATERIEL COMMAND
HANSCOM AIR FORCE BASE, MA 01731-3010

DTIC QUALITY INSPECTED 5

94-04232

Best Available Copy

"This technical report has been reviewed and is approved for publication."

JOSEPH W. SNOW
Chief, Satellite Meteorology Branch
Atmospheric Sciences Division

ROBERT A. McCLATCHEY
Director, Atmospheric Sciences Division

This report has been reviewed by the ESC Public Affairs Office (PA) and is releasable to the National Technical Information Service (NTIS).

"This technical report has been reviewed and is approved for publication."

REPORT DOCUMENTATION PAGE

Public reporting burden for this collection of information is estimated to average 1 hour per response, including the time for reviewing instructions, searching existing data sources, gathering and maintaining the data needed, and completing and reviewing the collection of information. Send comments regarding this burden estimate or any other aspect of this collection of information, including suggestions for reducing this burden, to Washington Headquarters Services, Directorate for Information Operations and Reports, 1215 Jefferson Davis Highway, Suite 1204, Arlington, VA 22202-4302, and to the Office of Management and Budget, Paperwork Reduction Project (0704-0188), Washington, DC 20503.

1. AGENCY USE ONLY (Leave blank)	2. REPORT DATE 19 July 1993	3. REPORT TYPE AND DATES COVERED Scientific, Interim

4. TITLE AND SUBTITLE
Sensitivity Analysis of the AVHRR Infrared Cirrus Model

5. FUNDING NUMBERS
PE 62101F
PR 6670
TA 17
WU 12

6. AUTHOR(S)

Allan J. Bussey and Robert P. d'Entremont

7. PERFORMING ORGANIZATION NAME(S) AND ADDRESS(ES)
Phillips Laboratory (GPAS)
29 Randolph Road
Hanscom AFB, MA 01731-3010

8. PERFORMING ORGANIZATION REPORT NUMBER

PL-TR—93-2166

ERP, No. 1126

9. SPONSORING/MONITORING AGENCY NAME(S) AND ADDRESS(ES)

10. SPONSORING/MONITORING AGENCY REPORT NUMBER

11. SUPPLEMENTARY NOTES

12a. DISTRIBUTION/AVAILABILITY STATEMENT

Approved for Public Release
Distribution Unlimited

12b. DISTRIBUTION CODE

13. ABSTRACT (Maximum 200 words)

We have studied the sensitivity to errors of a cirrus cloud analysis technique using NOAA Advanced Very High Resolution Radiometer (AVHRR) multispectral imagery. The sensitivity analysis reveals possible errors in computing optical depths and altitudes for nighttime cirrus cloud data samples taken from the First ISCCP Regional Experiment (FIRE) Phase I intensive field observations. The Appendix contains plots of the computed errors found in the study.

14. SUBJECT TERMS
AVHRR satellite imagery, Cirrus cloud, Cirrus altitude, Emissivity, Optical depth

15. NUMBER OF PAGES
42

16. PRICE CODE

17. SECURITY CLASSIFICATION OF REPORT	18. SECURITY CLASSIFICATION OF THIS PAGE	19. SECURITY CLASSIFICATION OF ABSTRACT	20. LIMITATION OF ABSTRACT
UNCLASSIFIED	UNCLASSIFIED	UNCLASSIFIED	UNLIMITED

Contents

Illustrations

Tables

1. INTRODUCTION

A cirrus cloud analysis technique using NOAA Advanced Very High Resolution Radiometer (AVHRR) multispectral imagery has been developed that determines the bulk radiative properties of cirrus clouds. This technique, called the AVHRR Infrared Cirrus model (AIRC), computes optical depths and altitudes for nighttime cirrus cloud data samples. Cirrus emissivities and altitudes are retrieved using a radiative transfer model that takes into account both the spectrally dependent transparent nature of thin cirrus clouds and the attenuative effects of atmospheric water vapor. The cirrus analysis technique capitalizes on the differences between the brightness temperatures of AVHRR Channels 3, 4, and 5 (3.7, 10.7, and 11.8 μm, respectively). For scenes that contain thin cirrus, the warmer underlying surface contributes significantly more energy to the Channel 3 satellite-measured radiance than to either Channel 4 or 5. These effects are included in AIRC and allow for the retrieval of cirrus emissivity and height. The multispectral cirrus analysis model demonstrates that more accurate thin cirrus altitudes can be obtained than those using single-channel longwave infrared techniques.

AIRC is restricted to nighttime AVHRR data because incident solar radiation entering the top of the Earth's atmosphere is not negligible at 3.7 μm and can, in fact, be as large as emitted terrestrial radiation, depending on the temperature (Smith and Rao, 1972). It is difficult to separate reflected solar from emissive thermal effects for daytime 3.7 μm measurements; this would comprise a study in itself. Researchers at the University of Utah are currently developing a daytime cirrus retrieval algorithm (Liou, personal communication).

1

A sensitivity analysis of the AIRC-retrieved cirrus parameters is important to users of the technique. It provides insight into how deviations in the correctness of surface temperature measurements, and also in the accuracy of Channel 3 and 4 brightness temperature measurements, can lead to errors in determining effective cirrus altitude and bulk emissivity. The methodology and results of the sensitivity analysis are the focus of this report.

2. NOTATION

$B_\lambda(T)$ Planck Blackbody Monochromatic Radiance,
Watts m^{-2} μm^{-1} ster^{-1} [ML^{-1}T^{-3}]

$B_j(T)$ Planck Spectrally-Averaged Blackbody Monochromatic Radiance for AVHRR Channel j, Watts m^{-2} μm^{-1} ster^{-1} [ML^{-1}T^{-3}]

ε Emissivity, Dimensionless

I_j Spectrally-Averaged Observed Upwelling Thermal Monochromatic Radiance Measured in AVHRR Channel j, Watts m^{-2} μm^{-1} ster^{-1} [ML^{-1}T^{-3}]

λ Wavelength, μm [L]

j   AVHRR Infrared Channel Number (j = 3, 4, 5)

r   Reflectivity, Dimensionless

$R_j(\lambda)$ Response Function at Wavelength λ for AVHRR Sensor j, Dimensionless

t   Transmissivity, Dimensionless

T	Temperature, K [θ]

τ	Atmospheric Transmittance, Dimensionless

z	Height AGL, km [L]

3. CIRRUS PROPERTY ANALYSIS METHOD

The spectrally-averaged upwelling thermal monochromatic radiance I_j measured by a downward pointing radiometer for a field of view filled completely with a non-reflective, thin cirrus cloud is well approximated by

$$
\begin{aligned}
I_j = {} & \epsilon_{j,cld} \, B_j(T_{cld}) \, \tau_j(z_{cld}) + \int_{z_{cld}}^{\infty} B_j(T) \, \frac{\partial \tau_j(z)}{\partial z} \, dz \\[2mm]
& + \epsilon_{j,sfc} \, B_j(T_{sfc}) \, \tau_j'(0) \, t_{j,cld} \, \tau_j(z_{cld}) \\[2mm]
& + \left[\int_{0}^{z_{cld}} B_j(T) \, \frac{\partial \tau_j'(z)}{\partial z} \, dz \right] t_{j,cld} \, \tau_j(z_{cld}) \,,
\end{aligned}
\tag{1a}
$$

where j is the AVHRR infrared (IR) Channel number; $\epsilon_{j,cld}$ is the cirrus cloud bulk emissivity for AVHRR Channel j; and $B_j(T)$ is defined by

$$
B_j(T) = \frac{\displaystyle \int_{\lambda_{j1}}^{\lambda_{j2}} B_\lambda(T) \, R_j(\lambda) \, d\lambda}{\displaystyle \int_{\lambda_{j1}}^{\lambda_{j2}} R_j(\lambda) \, d\lambda} \,,
\tag{1b}
$$

where $B_\lambda(T)$ is the monochromatic Planck radiance at wavelength λ for a blackbody at temperature T; $R_j(\lambda)$ is the AVHRR Channel j response function within the wavelength range $\lambda_{j1} \leq \lambda \leq \lambda_{j2}$ of sensor j; T_{dd} is the effective cirrus temperature; and $\tau_j(z)$ is the spectral transmittance for the atmospheric path between z and the top of the atmosphere at $z = \infty$, defined by

$$\tau_j(z) = \frac{\int_{\lambda_{j1}}^{\lambda_{j2}} \tau_\lambda(z) \, B_\lambda[T(z)] \, R_j(\lambda) \, d\lambda}{\int_{\lambda_{j1}}^{\lambda_{j2}} B_\lambda[T(z)] \, R_j(\lambda) \, d\lambda} \, , \qquad (1c)$$

where $\tau_\lambda(z)$ is the monochromatic transmittance for the path between level z and the top of the atmosphere at $z = \infty$; z_{dd} is the effective altitude of the cirrus cloud; $\varepsilon_{j,sfc}$ is the ground emissivity for Channel j; T_{sfc} is the ground skin temperature; $\tau_j'(z)$ is the spectral transmittance for the atmospheric path between level z and the cirrus cloud base (defined similarly as $\tau_j(z)$ above); and $t_{j,dd}$ is the cirrus cloud bulk transmissivity for AVHRR Channel j, j = 3, 4, 5.

The first term on the right side of Eq. (1a) denotes the cirrus cloud contribution to I_j. The second term denotes the upwelling emission by the atmosphere from the top of the cloud upward. The third term denotes that part of the upwelling radiance emitted by the underlying surface at z=0, attenuated by the atmosphere between the ground and the cloud, transmitted through the cloud, and attenuated finally by the atmosphere above the cloud. The fourth term denotes the upwelling radiance emitted by the atmosphere between the ground and the cloud, transmitted through the cloud, and attenuated again by the atmosphere above the cloud.

4

One important assumption that goes into the formulation of Eq. (1) is that the cirrus cloud is non-reflective. Ice particle cloud radiative properties computed by Hunt (1973) indicate that cirrus reflectivities are very small; for an optically thick cloud the Channel 3 (3.7μm) cirrus reflectivity $r_{3,cld}$ never exceeds 0.02, and Channels 4 and 5 (10.7 and 11.8μm, respectively) reflectivities never reach 0.01. Thus for cirrus clouds the energy conservation equation is well approximated by

$$\epsilon_{j,cld} + t_{j,cld} = 1 \; ,$$

or

$$t_{j,cld} = 1 - \epsilon_{j,cld} \; , \qquad j = 3, 4, 5. \qquad (2)$$

Although the cirrus reflectivities are effectively zero for Channels 3, 4, and 5, the emissivities are not as easily handled. Equation (2) governs the radiative properties of cirrus clouds for each channel individually, but offers no information on how the emissivities for a particular cirrus cloud can vary from channel to channel. Table 1 lists a set of corresponding emissivities for cirrus clouds of varying thicknesses, and composed of spherical ice particles with a particle size mode radius of 16 μm (after Hunt, 1973). Note how the 3.7μm Channel 3 cloud emissivities are never larger than the 10.7μm Channel 4 emissivities. It is possible to construct a simple linear regression equation between the Channel 3 and Channel 4 transmissivities of the form

$$\ln t_{3,cld} = m \ln t_{4,cld} + \ln K \; , \qquad (3)$$

Table 1. Corresponding Values of Emissivities for AVHRR Channels 3 and 4, Listed as a Function of Cloud Thickness. The Cloud is Assumed to be Composed of Spherical Ice Particles, and a Modified Gamma Size Distribution is Used With a Minimum Droplet Radius of 0.1μm, a Maximum of 25μm, and a Mode Radius of 16μm; Number Density is 100 cm^{-3} (After Hunt, 1973)

Cloud Thickness (m)	Channel 3 Emissivity $\varepsilon_{3,cld}$	Channel 4 Emissivity $\varepsilon_{4,cld}$
0.5	.024	.047
1	.048	.091
1.5	.071	.127
2	.095	.175
3	.140	.235
4	.192	.299
5	.241	.355
10	.407	.593
20	.659	.849
30	.810	.934
40	.901	.973
50	.931	.988
100	.971	.995
500	.979	.996

where m and ln K are the regression slope and intercept values, respectively, in log-log space. Performing the regression analysis on the transmissivity pairs $(1-\varepsilon_{4,cld}, 1-\varepsilon_{3,cld})$ given in Table 1 for m and ln K and solving Eq. (3) for $\varepsilon_{3,cld}$ yields K=1 and m=0.67, or

$$\varepsilon_{3,cld} = 1 - (1 - \varepsilon_{4,cld})^{0.67} . \tag{4a}$$

The correlation coefficient for Eq. (4a) is 0.997. This equation allows the Channel 3 cirrus emissivity to be determined once the corresponding Channel 4 emissivity is known. The emissivities of Channels 4 and 5 are more similar since they represent spectral bands that lie close to each other in the longwave IR window. After Inoue (1987) it is assumed that K=1 and m=1.08, so that

$$\varepsilon_{5,cld} = 1 - (1 - \varepsilon_{4,cld})^{1.08} , \tag{4b}$$

which reproduces differences between Channels 4 and 5 brightness temperatures in the range observed by Saunders and Kriebel (1988) for thin cirrus.

Consider a pixel for which the atmospheric temperature-moisture profile and underlying surface skin temperature T_{sfc} are known. Then the transmittance profiles $\tau_j(z)$ and $\tau_j'(z)$ can be computed using a multivariate polynomial regression transmittance model developed for AVHRR thermal channels by Weinreb and Hill (1980). In fact, all terms on the right side of Eq. (1) would then be either known or computable. Using Eq. (2) to rewrite the cirrus transmissivity $t_{j,cld}$ in terms of the emissivity $\varepsilon_{j,cld}$, and using Eq. (4) to express the Channels 3 and 5 emissivities as a function of the Channel 4 emissivity $\varepsilon_{4,cld}$, the satellite-measured radiance I_j can be computed as a function

7

$$I_j = I_j \, (\, z_{cld} \, , \, \epsilon_{4,cld} \,) \, , \qquad j = 3, 4, 5 \qquad\qquad (5a)$$

using Eq. (1). In Eq. (5a), the upwelling radiance I_j is explicitly expressed as a function of the effective cloud altitude z_{cld} and the Channel 4 cirrus bulk emissivity $\epsilon_{4,cld}$. The observed radiances I_j can be converted to observed brightness temperature T_j using a relationship similar to Eq. (1b), so that

$$T_j = T_j \, (\, z_{cld} \, , \, \epsilon_{4,cld} \,) \, , \qquad j = 3, 4, 5 \, . \qquad\qquad (5b)$$

A sample set of brightness temperature calculations T_3, T_4, and T_5 are plotted in Table 2 as a function of z_{cld} and $\epsilon_{4,cld}$ for an atmospheric sounding taken at Madison, Wisconsin on 28 October 1986 at approximately 0930 UTC. The surface skin temperature T_{sfc} was chosen to be 278.4 K (this is 1.5 K lower than the ambient air temperature of the lowest atmospheric layer, a condition common at night), and the ground emissivities $\epsilon_{3,sfc}$, $\epsilon_{4,sfc}$, and $\epsilon_{5,sfc}$ were chosen to be 0.95, 1, and 1, respectively. Note in general that for a fixed brightness temperature measurement T_j, cirrus altitude decreases as emissivity increases.

It is possible to use real-time computations similar to those summarized in Table 2 in conjunction with simultaneously measured satellite brightness temperatures for a particular thin cirrus field of view in order to infer the cirrus effective cloud height, emissivities, and transmissivities. This is accomplished by comparing the measured AVHRR brightness temperatures to the tabulated ones. Consider the Table 2 brightness temperatures to be representative of a hypothetical cirrus cloud scene. Suppose in addition that the scene's satellite-measured brightness temperatures for Channels 3, 4, and 5 are 267.1, 256.4, and 254.7 K, respectively. Upon comparison of these brightness temperatures with the corresponding temperatures listed in Table 2, the effective cloud height/emissivity pair

8

simultaneously consistent with the brightness temperature measurements is $z_{cld} = 8$ km and $\varepsilon_{4,cld} = 0.6$. From Eq. (4a), the corresponding Channel 3 cirrus emissivity $\varepsilon_{3,cld}$ is 0.46, and from Eq. (4b), $\varepsilon_{5,cld}$ is 0.63. Using Eq. (2), the cirrus transmissivities $t_{3,cld}$, $t_{4,cld}$, and $t_{5,cld}$ are 0.54, 0.40, and 0.37, corresponding to optical depths $\delta_{3,cld}$, $\delta_{4,cld}$, and $\delta_{5,cld}$, of 0.62, 0.92, and 0.99, respectively ($\delta_{j,cld} \approx -\ln t_{j,cld}$).

Figure 1 contains a contouring of the theoretical brightness temperatures T_4 (listed in Table 2) as a function of emissivity and effective cirrus altitude. Note how a Channel 4 brightness temperature T_4 of 260 K constrains the cirrus emissivity to be greater than ~0.4, and the cirrus altitude to be higher than ~5 km. Figure 2 contains a contouring of the theoretical brightness temperature differences listed in Table 2 between Channels 3 and 4, plotted as a function of emissivity and cirrus altitude. Note how the difference is at a maximum for relatively high values of emissivity and altitude (for example, $T_3 - T_4 > 26$ K for an emissivity of 0.9 and an altitude of 12 km).

For a pair of coincident AVHRR brightness temperature measurements T_3 and T_j ($j = 4$ or 5), a set of two equations in two unknowns z_{cld} and $\varepsilon_{4,cld}$ can be generated using Eq. (5b). Simultaneous solution of these two equations using a simple graphical technique yields the (z_{cld}, $\varepsilon_{4,cld}$) pair that corresponds to the measurements T_3 and T_j. Then using Eq. (4a) for $j=4$ and (4b) for $j=5$ the Channel 3 and Channel 5 cirrus emissivities can be obtained. Once $\varepsilon_{3,cld}$ and $\varepsilon_{j,cld}$ are determined, Eq. (2) can be applied to calculate the cirrus transmissivities $t_{3,cld}$ and $t_{j,cld}$ and the approximation

$$\delta_{j,cld} \approx -\ln t_{j,cld} \tag{6}$$

can be used to estimate the cirrus bulk optical depth $\delta_{j,cld}$.

9

Table 2. Channels 3, 4, and 5 Brightness Temperature Measurements for Various Effective Cloud Top Heights and Channel 4 Emissivities, Calculated Using Eqs. (1) and (4) for the Madison, Wisconsin Sample Atmosphere.

Effective Cloud Height z_{cld} (km)	Channel 4 Cirrus Emissivity $\varepsilon_{4,cld}$					
	0	0.2	0.4	0.6	0.8	1.0
Theoretically-Expected Brightness Temperatures T_3 for AVHRR Channel 3 (K)						
12	277.5	274.5	270.9	265.9	257.8	212.3
10	277.5	274.6	271.0	266.1	258.3	220.8
8	277.5	274.8	271.5	267.1	260.3	237.1
6	277.5	275.3	272.8	269.5	264.9	253.5
4	277.5	276.3	274.9	273.3	271.2	267.1
2	277.5	277.6	277.8	278.0	278.2	278.6
0	277.5	277.8	278.2	278.6	279.0	279.8
Theoretically-Expected Brightness Temperatures T_4 for AVHRR Channel 4 (K)						
12	278.6	269.2	258.6	246.5	231.8	212.3
10	278.6	270.0	260.4	249.5	236.8	220.8
8	278.6	271.8	264.4	256.4	247.4	237.1
6	278.6	274.1	269.4	264.4	259.1	253.5
4	278.6	276.4	274.2	271.9	269.5	267.1
2	278.6	278.6	278.6	278.6	278.6	278.6
0	278.6	278.9	279.2	279.4	279.7	279.9
Theoretically-Expected Brightness Temperatures T_5 for AVHRR Channel 5 (K)						
12	278.5	267.9	256.4	243.5	228.8	212.3
10	278.5	268.9	258.4	247.0	234.4	220.8
8	278.5	271.0	263.1	254.7	245.9	237.1
6	278.5	273.6	268.6	263.5	258.3	253.4
4	278.5	276.1	273.8	271.4	269.1	266.9
2	278.5	278.4	278.4	278.3	278.2	278.1
0	278.5	278.8	279.0	279.3	279.5	279.7
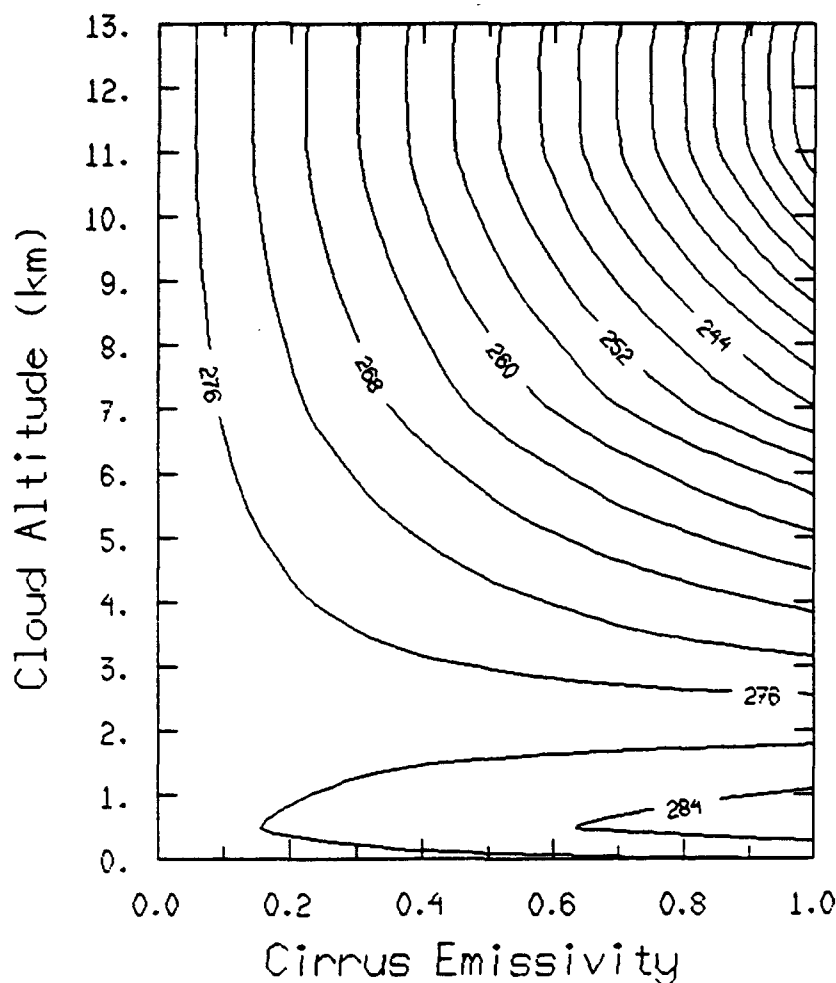
Figure 1. AVHRR 10.7μm Channel 4 Theoretical Brightness Temperatures as a Function of the Channel 4 Emissivity $\varepsilon_{4,cld}$ and the Effective Cirrus Altitude z_{cld}

4. SENSITIVITY ANALYSIS METHOD

The objective of the remainder of this report is to test the AVHRR infrared cirrus model for retrieved emissivity and effective cloud height accuracy when introducing known errors into the independent variables used to run the model. Table 2 shows expected brightness temperatures for AVHRR Channels 3, 4, and 5 in K, for various effective cloud heights and Channel 4 emissivities. Clearly, errors in measuring the brightness temperatures will cause reduced accuracy in the resultant effective cloud height and cirrus bulk emissivity. As can be seen in Figure 1, the range of values in observed brightness temperature, over the range of effective cloud height from 0 to 12 km, increases as Channel 4 cirrus emissivity increases from 0 to

11

1.0. But this is not a quantifiable indication of where the greatest error may occur. Vigorous testing is necessary in order to determine where the AIRC model is most sensitive. The surface temperature T_{sfc} has a significant influence on the model as well as the aforementioned AVHRR brightness temperature measurements T_3, T_4, and T_5. The sensitivity analysis takes into account errors in T_3 and T_4 and the surface temperature T_{sfc}, and yields error ranges of emissivity and effective cloud altitudes. The following error values were examined:

ΔT_{sfc} = 0, +3, -3 (K) (precise, 3 K too high, and 3 K too low, respectively);

$\Delta T_3 = T_3$ Measurement Error = 0, +1, +2, +3, +4, +5, -1, -2, -3, -4, -5 (K); and

$\Delta T_4 = T_4$ Measurement Error = 0, +1, +2, +3, +4, +5, -1, -2, -3, -4, -5 (K).

The true effective cirrus altitudes were limited to 7, 9, and 11 km and to control the test size, Channel 4 emissivities were investigated at 0.2, 0.5, and 0.9, ranging from optically thin to nearly opaque. Finally, the Fort McCoy, 28 October 1986, FIRE radiosonde data were used in running the Weinreb and Hill transmittance model. The results of the sensitivity analysis are presented in the next section.

5.   SENSITIVITY ANALYSIS

The summary descriptive statistics of the overall sensitivity analysis are listed in Tables 3, 4, and 5. A quick comparison shows that the largest errors occur at low values of emissivity (ε_4 = 0.2) and dramatically decrease in magnitude at high emissivity values (ε_4 = 0.9). At a given emissivity, induced errors in the surface temperature have little effect on the magnitude of the resultant deviations from expected values of cloud altitude and emissivity. These results are useful, but to obtain a better quantitative understanding of exactly how these variations are taking place, we plotted the data on equal-area charts of T_3 and T_4 errors ΔT_3 and ΔT_4,

12

respectively, as a function of height and emissivity (see Figures 2-10, Appendix A). The following sections describe the information contained in these plots.

Table 3. $\varepsilon_4 = 0.20$; ΔT_3 and $\Delta T_4 = \pm 5$ K Where: T_{sfc} is the Surface Temperature (K); z_{cld} is the Effective Cloud Altitude (km); $\Delta\varepsilon_4$ is the Resulting Difference (+ or -) in Channel 4 Emissivity From Expected Values; and Δz is the Resulting Difference (+ or -) in Altitude (km) From Expected Values.

ΔT_{sfc} (K)	z_{cld} (km)	MAX $\Delta\varepsilon_4$		MAX Δz		AVG $\Delta\varepsilon_4$		AVG Δz	
		+	-	+	-	+	-	+	-
277.1 ($\Delta T_{sfc}=+3$)	7.0	.79	.20	5.5	7.0	.29	.16	3.6	4.9
	9.0	.75	.20	3.5	9.0	.32	.15	2.5	5.7
	11.0	.75	.20	1.5	11.0	.32	.16	1.4	7.0
274.1 ($\Delta T_{sfc}=0$)	7.0	.74	.20	5.5	7.0	.26	.16	3.7	4.8
	9.0	.77	.20	3.5	9.0	.31	.15	2.2	5.7
	11.0	.78	.20	1.5	11.0	.31	.16	1.3	6.8
271.1 ($\Delta T_{sfc}=-3$)	7.0	.76	.20	5.5	7.0	.26	.16	3.6	5.6
	9.0	.78	.20	5.5	9.0	.31	.15	3.4	5.6
	11.0	.79	.20	1.5	11.0	.30	.16	1.4	6.7

Table 4. $\varepsilon_4 = 0.50$; ΔT_3 and $\Delta T_4 = \pm 5$ K Where: T_{sfc} is the Surface Temperature (K); z_{cld} is the Effective Cloud Altitude (km); $\Delta\varepsilon_4$ is the Resulting Difference (+ or -) in Channel 4 Emissivity From Expected Values; and Δz is the Resulting Difference (+ or -) in Altitude (km) From Expected Values.

ΔT_{sfc} (K)	z_{cld} (km)	MAX $\Delta\varepsilon_4$		MAX Δz		AVG $\Delta\varepsilon_4$		AVG Δz	
		+	-	+	-	+	-	+	-
277.1 ($\Delta T_{sfc}=+3$)	7.0	.49	.35	5.5	3.0	.28	.21	3.8	1.7
	9.0	.45	.28	3.5	4.0	.19	.16	2.7	2.1
	11.0	.35	.25	1.5	5.0	.13	.14	1.5	2.4
274.1 ($\Delta T_{sfc}=0$)	7.0	.46	.38	5.5	2.5	.28	.23	3.9	1.5
	9.0	.46	.29	3.5	3.9	.21	.16	2.7	2.1
	11.0	.37	.26	1.5	4.9	.14	.15	1.4	2.4
271.1 ($\Delta T_{sfc}=-3$)	7.0	.50	.41	5.5	2.5	.31	.24	3.8	1.5
	9.0	.48	.30	3.5	3.5	.22	.17	2.7	2.0
	11.0	.39	.26	1.5	4.7	.14	.15	1.5	2.3

Table 5. $\varepsilon_4 = 0.90$; ΔT_3 and $\Delta T_4 = \pm 5$ K Where: T_{sfc} is the Surface Temperature (K); z_{cld} is the Effective Cloud Altitude (km); $\Delta\varepsilon_4$ is the Resulting Difference (+ or -) in Channel 4 Emissivity From Expected Values; and Δz is the Resulting Difference (+ or -) in Altitude (km) From Expected Values.

ΔT_{sfc} (K)	z_{cld} (km)	MAX $\Delta\varepsilon_4$		MAX Δz		AVG $\Delta\varepsilon_4$		AVG Δz	
		+	-	+	-	+	-	+	-
	7.0	.09	.20	2.8	1.0	.03	.09	0.4	0.5
277.1	9.0	.04	.10	2.2	0.9	.02	.06	0.6	0.4
(ΔT_{sfc}=+3)	11.0	.02	.07	1.5	1.1	.01	.04	1.3	0.5
	7.0	.10	.24	3.1	1.0	.04	.10	0.8	0.5
274.1	9.0	.05	.12	3.5	1.0	.02	.06	0.7	0.5
(ΔT_{sfc}=0)	11.0	.02	.07	1.5	1.1	.01	.04	1.1	0.5
	7.0	.09	.27	3.4	1.0	.04	.12	0.8	0.5
271.1	9.0	.06	.13	3.5	1.0	.02	.06	0.7	0.5
(ΔT_{sfc}=-3)	11.0	.03	.07	1.5	1.1	.01	.04	1.3	0.5

6. SENSITIVITY RESULTS FOR OPTICALLY THIN CIRRUS CLOUDS: AVHRR CHANNEL 4 EMISSIVITY OF 0.2

6.1 Surface Temperature of 277.1 K

This section describes the sensitivity analysis results plotted in Figure 2, Appendix A.

When the surface temperature value is in error by +3 K there are large errors in retrieved emissivity (ε) and cloud height (z) for low, medium, and high cloud altitudes. The largest emissivity errors occur where the T_3 and T_4 errors are both negative at low altitudes (7 km) but shift to where T_3 errors are negative and T_4 errors are positive at medium (9 km) and high altitudes (11 km). In general, negative

15

errors in T_3 result in a positive ε error and positive errors in T_3 result in a negative ε error regardless of the magnitude of the T_4 error ΔT_4. As the positive T_3 error increases, the ε value decreases and goes to 0.00 for $\Delta T_3 \geq +3$ K. Calculated emissivity values range from 0.00 to 0.99 at 7 km cloud heights and 0.00 to 0.95 at 9 km and 11 km cloud heights.

Cirrus height errors are present for all T_3 and T_4 error values but become more negative as the true cloud altitude increases. At 7 km, z_{cld} errors are predominantly negative when both ΔT_3 and ΔT_4 are negative, and are predominantly positive when ΔT_4 is positive and ΔT_3 is negative. At 9 and 11 km, z_{cld} errors are mostly negative when T_3 errors are negative for both positive and negative errors of T_4. Cloud altitude errors Δz_{cld} are generally positive for $0 \leq \Delta T_3 \leq 2$ K, and for positive and negative errors in T_4; whereas there is no cirrus cloud detected for $\Delta T_3 \geq +3$ K, which results in large z_{cld} errors. Calculated cirrus height values range from 0 to 12.5 km for all cloud altitudes and z_{cld} errors increase in magnitude as the cloud altitude increases.

6.2   Surface Temperature of 274.1 K

This section describes the sensitivity analysis results plotted in Figure 3, Appendix A.

If there is no error in the surface temperature (that is, $\Delta T_{sfc} = 0$ K), the emissivity errors that occur are remarkably consistent for all cloud altitudes when errors are introduced in T_3 and T_4. Errors in emissivity are positive for $\Delta T_3 < 0$ K and they are negative for $\Delta T_3 > 0$ K. The largest positive ε errors occur where T_3 and T_4 errors are both negative for a cloud altitude of 7 km; they occur for $-3 \leq \Delta T_4 \leq 3$ K for 9 km cloud altitude; and they occur when $\Delta T_3 < 0$ K and $\Delta T_4 > 0$ K at 11 km cloud

16

altitude. The calculated ε values go to 0.0 for T_3 errors exceeding +3 K. The range of ε errors is from approximately -0.20 to +0.75 for all cloud altitudes.

Height errors at T_{sfc} = 274.1 K (that is, at ΔT_{sfc} = 0 K) are very similar to height errors at 277.1 K (ΔT_{sfc} = +3 K). They become increasingly negative as the true cloud altitude increases from 0 to 12.5 km. Cloud height errors are generally positive for T_3 errors between 0 and +2 K, and for both positive and negative errors in T_4. The largest negative Δz_{cld} occurs for $\Delta T_3 \geq$ +3 K since no cirrus would be detected at all.

6.3   Surface Temperature of 271.1 K

This section describes the sensitivity analysis results plotted in Figure 4, Appendix A.

Emissivity errors are generally similar at 7, 9, and 11 km cloud altitudes when the surface temperature is in error by -3 K (T_{sfc} = 277.1 K); however there are some distinct differences. Emissivity errors $\Delta \varepsilon$ are positive for negative T_3 errors at all cloud altitudes with the exception of 7 km, which fails to detect cirrus at T_4 error values of +5 K. Cirrus is also not detected for all cloud altitudes where $\Delta T_3 \geq$ +3 K. Maximum positive $\Delta \varepsilon$ errors occur at 7 km cloud altitudes when T_3 and T_4 errors are both negative but shift to where T_3 errors are negative and T_4 errors are positive at 9 and 11 km cloud altitude. Emissivity values range from 0.00 to 0.96 for each of the cloud altitudes.

At 7 km true cirrus altitude, height errors Δz_{cld} are largest when T_4 = +5 K and for $\Delta T_3 \geq$ +3 K; this is where the AIRC model would fail to detect cirrus. The model would also fail to detect cirrus at T_3 error values $\geq$ +3 K for 9 and 11 km true altitudes, resulting in large negative height errors. As the true cloud altitude z_{cld} increases from 7 to 11 km the errors become more negative and increase in

magnitude from -2.8 to -6.6 K. The range of negative height errors is from 0 to -7.0, -9.0, and -11.0 km corresponding to cloud altitudes of 7, 9, and 11 km respectively. At each altitude the error values are generally positive for T_3 error values between 0 and +2 K.

7.   SENSITIVITY RESULTS FOR OPTICALLY MODERATE CIRRUS CLOUDS: AVHRR CHANNEL 4 EMISSIVITY OF 0.5

7.1   Surface Temperature of 277.1 K

This section describes the sensitivity analysis results plotted in Figure 5, Appendix A.

For ΔT_{sfc} = +3 K, emissivity errors are similar for each of the three true cloud altitudes z_{cld} = 7, 9, and 11 km. Positive emissivity errors $\Delta \varepsilon_4$ increase as T_3 negative errors increase, and negative $\Delta \varepsilon$ errors increase as T_3 positive errors increase. The positive ε errors also increase as T_4 errors increase from negative to positive values. There is little variation in negative ε errors as T_4 errors vary, especially at z_{cld} = 11 km altitude. However, there is a small increase in negative ε errors as T_4 errors decrease from positive to negative values. Positive ε errors range from 0.00 to 0.49 at z_{cld} = 7 km, 0.00 to 0.45 at 9 km, and 0.00 to 0.35 at 11 km; while negative ε errors have a maximum of -0.35 at 7 km, -0.28 at 9 km, and -0.25 at 11 km.

Height errors generally become more positive as ΔT_3 increases positively, and become more negative as ΔT_3 increases negatively for 7, 9, and 11 km cloud altitudes. The height errors also increase in a positive manner as T_4 errors decrease for each cloud altitude. The magnitude of error for cirrus height ranges from Δz_{cld} = -3.0 to +5.5 km at 7 km; from -4.0 to +3.5 km at 9 km; and from -5.0 and +1.5 km at 11 km.

18

7.2   Surface Temperature of 274.1 K

This section describes the AIRC sensitivity analysis results plotted in Figure 6, Appendix A.

For ΔT_{sfc} = 0 K, emissivity errors at 274.1 K surface temperature are similar to the emissivity errors discussed for ΔT_{sfc} = -3 K (Section 7.1). Positive ε errors increase in magnitude as T_3 negative errors increase in magnitude, and negative ε errors increase as T_3 positive errors increase. The positive ε errors also increase as T_4 errors increase while there is little change in negative ε errors with negative changes in T_4 error. The magnitude of positive ε errors ranges from 0.00 to 0.46 at 7 km and 9 km true cirrus altitudes and from 0.00 to 0.37 at 11 km true cirrus altitude. The magnitude of the negative ε errors decreases slightly from -0.38 at z_{dd} = 7 km cirrus altitude to -0.26 at z_{dd} = 11 km cirrus altitude.

Height errors become more positive as positive ΔT_3 increases, for all cirrus altitudes and for 274.1 K surface temperature. Height errors Δz_{dd} become more negative as positive T_4 error differences increase at 7 and 9 km cirrus altitude where T_3 temperature differences are less than +4 K and at z_{dd} = 11 km altitude where T_3 temperature differences are less than +3 K. Height errors reach a maximum of +5.5 km for all $\Delta T_3 \geq 4$ K at 7 km cirrus altitude; Δz_{dd} = +3.5 km for all $\Delta T_3 \geq 4$ K at 9 km cirrus altitude; and Δz_{dd} = +1.5 km for all $\Delta T_3 \geq +3$ K at 11 km cirrus altitude. Minimum height error values range from -2.5 km at 7 km; -3.9 km at 9 km; and -4.9 km at 11 km cirrus effective altitudes.

7.3   Surface Temperature of 271.1 K

This section describes the AIRC sensitivity analysis results plotted in Figure 7, Appendix A.

19

Emissivity errors at 271.1 K surface temperature $\Delta T_{sfc} = -3$ K are similar at 9 and 11 km cirrus altitude and are also similar to the emissivity pattern found at 274.1 and 277.1 K surface temperature. For these two altitudes, emissivity errors become more positive as T_3 errors become more negative and T_4 errors become more positive. Emissivity errors become more negative as T_3 errors increase positively. However, at $z_{dd} = 7$ km altitudes, $\Delta \varepsilon$ becomes more positive as T_3 errors become more negative, and emissivity errors become more positive as T_4 errors become more positive for all ΔT values except for $\Delta T_3 = -5$ K and $\Delta T_4 = +5$ K. At this point the emissivity error $\Delta \varepsilon$ decreases instead of increasing. Also, at all values of $\Delta T_4 = +5$ K, the $\Delta \varepsilon$ is positive. At values of $\Delta T_4 < +5$ K, ε errors range from -0.30 to +0.48 at 7 km cirrus altitude; from -0.41 to +0.48 at 9 km cirrus altitude; and from -0.26 to +0.39 at 11 km cirrus altitude.

Height errors at 9 and 11 km cirrus altitude are very similar. At $z_{dd} = 9$ km altitude, Δz errors decrease from a maximum of +3.5 km to a minimum of -3.5 km as T_3 error values decrease and T_4 error values increase. At 11 km altitude, Δz errors decrease in the same way as at 9 km altitude but from a maximum of +1.5 km to a minimum of -4.7 km. The Δz error is constant at +3.5 km for $\Delta T_3 \geq +4$ K and 9 km altitude and constant at +1.5 km for $\Delta T_3 \geq +3$ K at 11 km altitude, independent of T_4 error values. At 7 km cirrus altitude, Δz error values range from a maximum of +5.5 km to a minimum of -2.5 km. The Δz error values become more negative as T_3 errors decrease and T_4 errors increase, with the exception of one point at $\Delta T_3 = -5$ K and $\Delta T_4 = +5$ K where the altitude error changes from -1.5 km to +1.5 km. The Δz errors do not remain constant for any values of ΔT_3 and ΔT_4 at 7 km altitude, as they sometimes did for higher true cirrus altitudes.

20

8.   SENSITIVITY RESULTS FOR OPTICALLY THICK CIRRUS CLOUDS: CHANNEL 4 EMISSIVITY OF 0.9

8.1   Surface Temperature of 277.1 K

This section describes the AIRC sensitivity analysis results plotted in Figure 8, Appendix A.

For ΔT_{sfc} = +3 K, emissivity error values are very similar for all altitude levels when ε_4 = 0.9. In general, positive ε errors occur for $\Delta T_3 < 0$ K and negative ε errors occur for $\Delta T_3 > 0$ K. At z_{dd} = 7 km, positive $\Delta \varepsilon$ values range from 0.00 to 0.09; while negative error values range from 0.00 to -0.27. The largest negative ε error occurs as T_4 values increase negatively. Positive ε errors increase slightly as T_4 values become more positive. Emissivity errors are almost symmetrical at z_{dd} = 9 km and range from 0.06 to 0.13. At 11 km, the ε errors are symmetrical and values range from -0.07 to 0.03, indicating a very high level of tolerance for measurement error for optically thick cirrus clouds.

Cirrus height errors Δz_{dd} show strong similarity for each altitude examined. Height errors become more positive as T_4 values decrease for 7, 9, and 11 km altitudes. The Δz error values range from -1.0 to +3.4 km at z_{dd} = 7 km altitude; from -1.0 to +3.5 km at 9 km altitude; and from -1.1 to +1.5 km at 11 km altitude. In general about 40% of the Δz error values are negative and the remainder are either zero or positive.

8.2   Surface Temperature of 274.1 K

This section describes the AIRC sensitivity analysis results plotted in Figure 9, Appendix A.

Emissivity errors are small for $\Delta T_{sfc} = 0$ K, and vary in a similar manner as at $\Delta T_{sfc} = +3$ K. Emissivity errors vary from positive to negative as ΔT_3 values go from negative to positive at 7, 9, and 11 km true altitudes. Emissivity error values range from -0.24 to +0.10 at 7 km; from -0.12 to +0.05 at 9 km; and from -0.07 to +0.02 at 11 km. The values become more positive at $z_{dd} = 7$ km as ΔT_4 values become more positive and show little variation at 9 and 11 km altitudes.

Cirrus height errors vary similarly for each of the three altitudes, in much the same way as the variation described for 277.1 K surface temperatures. The Δz errors become more positive as ΔT_4 values decrease for each altitude. Values of Δz_{dd} range from -1.0 to +3.1 km at 7 km true cirrus altitude; from -1.0 to +3.5 km at 9 km altitude; and from -1.0 to + 1.5 km at 11 km altitude.

8.3   Surface Temperature of 271.1 K

This section describes the AIRC sensitivity analysis results plotted in Figure 10, Appendix A.

Overall, the smallest errors in emissivity occur at 271.1 K surface temperature where $\varepsilon_4 = 0.9$. Values of $\Delta\varepsilon$ range from -0.20 to +0.09 at 7 km true cirrus altitude; from -0.10 to + 0.04 at 9 km altitude; and from -0.07 to +0.02 at 11 km altitude. At $z_{dd} = 7$ km, there is a small positive increase in emissivity error values as T_4 temperature errors become more positive, but very little change in ε error values occurs as ΔT_4 values change at both 9 and 11 km. Again, values of ε error are positive where ΔT_3 values are negative and are negative where ΔT_3 values are positive.

Overall, the height error values Δz_{dd} are also the smallest for 271.1 K surface temperature and $\varepsilon_4 = 0.9$. Values of Δz_{dd} range from -1.0 to +2.8 km at $z_{dd} = 7$ km

22

true altitude; from -0.9 to +2.2 km at z_{dd} = 9 km altitude; and from -1.1 to +1.5 km at z_{dd} = 11 km altitude. In general, Δz error values are negative where ΔT_4 values are positive and are positive where ΔT_4 values are negative. The variation in Δz error values is very similar to those discussed earlier for ε_4 = 0.9 at 277.1 K and 274.1 K surface temperatures.

9. SUMMARY

In general, retrieved emissivity and altitude errors are greatest when the true cirrus emissivity ε_4 is low, and least when ε_4 is high. Therefore, the AIRC cirrus model is least sensitive to T_3 and T_4 measurement errors when the cirrus is optically thick. Errors in both effective emissivity and altitude ($\Delta\varepsilon$ and Δz_{dd} respectively) are greatest at ε_4 = 0.2 (optically thin cirrus). In all cases the errors decrease as the true altitude z_{dd} increases from 7 km to 11 km. The errors also tend to decrease as the surface temperature values increase from -3 K to +3 K of the true T_{sfc} value. Finally, less variation in error occurs for higher than for lower ε_4 values and in general the largest error values occur at ε_4 = 0.2.

These error tendencies are, in part, due to the constraints placed on cirrus attributes by AIRC. The decrease in altitude error from 7 to 11 km is affected by the limitation of a 12.5 km height for cirrus clouds imposed by the model. Also, it is logical for the largest errors to occur for the optically thinnest cirrus (ε_4 = 0.2), since the measured AVHRR brightness temperatures are minimally affected by the cloud itself.

Somewhat surprisingly, the accuracy of the surface skin temperature T_{sfc} turns out to be one of the less sensitive aspects of the AIRC cirrus model.

Surface emissivities $\varepsilon_{j,sfc}$ can be very difficult to specify, especially for the 3.7 μm Channel 3. Aside from a dominant wavelength dependence, $\varepsilon_{j,sfc}$ varies on local

and even subpixel scales due to effects such as variable soil moisture content, urban/rural mixed fields of view, vegetation cover, and the like. Cirrus cloud emissivities and transmissivities have complex dependencies on wavelength, particle size distribution, and ice particle shapes. Errors in the vertical temperature profile or the atmospheric transmittances will manifest themselves largely in the accuracy of the retrieved cloud heights; the effect on clear-column radiance computations is small since each of the three AVHRR IR channels lie within reasonably clean atmospheric windows.

Sources of error in measured brightness temperature can stem from the use of AVHRR local-area coverage (LAC) 1 km data. LAC footprints from one AVHRR channel to the next are usually not precisely aligned, meaning that the "coincident" brightness temperature measurements T_3, T_4, and T_5 might not be from precisely the same FOV. One way to alleviate this problem is to average a set of 3 x 3 or 4 x 4 LAC pixels together before inserting them into the AIRC cirrus algorithm. Care would have to be exercised, however, to ensure that each of the pixels being averaged is completely filled with cirrus. (This is an important assumption of the AIRC model.) Finally, Channel 3 is known to be somewhat noisy; again, this problem may be alleviated through the application of spatial averaging techniques.

Special thanks is given to Dr. Michael K. Griffin (PL/GPAS) who provided the program used in generating the plots of Appendix A. The most effective use of this report is for AIRC cirrus model users to refer to these plots for a perception of possible errors inherent in the model retrieval results.

Bibliography

Hunt, Garry E., 1973: Radiative Properties of Terrestrial Clouds at Visible and Infra-Red Thermal Window Wavelengths. *Quart. J. Royal Meteor. Soc.*, **99**, 346- 369.

Inoue, Toshiro, 1987: A Cloud Type Classification With NOAA-7 Split-Window Measurements. *J. Geophys. Res.*, **92**, No. D4, 3991-4000.

Saunders, R. W. and K. T. Kriebel, 1988: An Improved Method for Detecting Clear Sky and Cloudy Radiances from AVHRR Data. *Int. J. Remote Sensing*, **9**, 123-150.

Smith, W. L., and P. K. Rao, 1972: The determination of surface temperature from satellite 'window' radiation measurements. Temperature: Its Measurement and Control in Science and Industry. 4th Symp. on Temperature, 1971, Washington, D.C. Instrument Soc. of Amer., 2251-2257.

Weinreb, Michael P. and Michael L. Hill, 1980: *Calculation of Atmospheric Radiances and Brightness Temperatures in Infrared Window Channels of Satellite Radiometers.* NOAA Tech. Rep. NESS 80, U.S. Dept. of Commerce, Washington D.C., 40 pp.

APPENDIX A

PLOTS OF AIRC SENSITIVITY ANALYSIS RESULTS AS A FUNCTION OF T_3 AND T_4 MEASUREMENT ERRORS
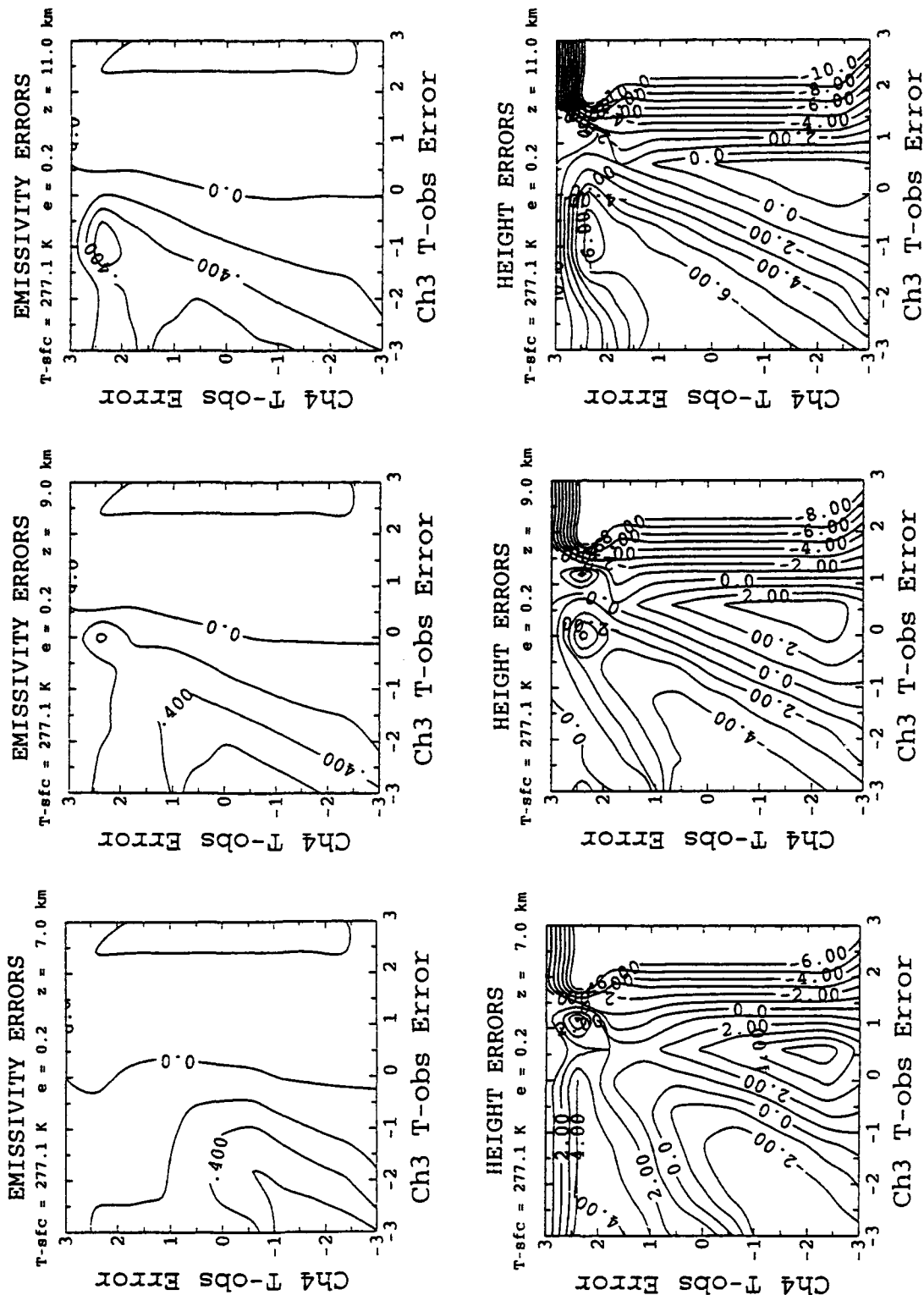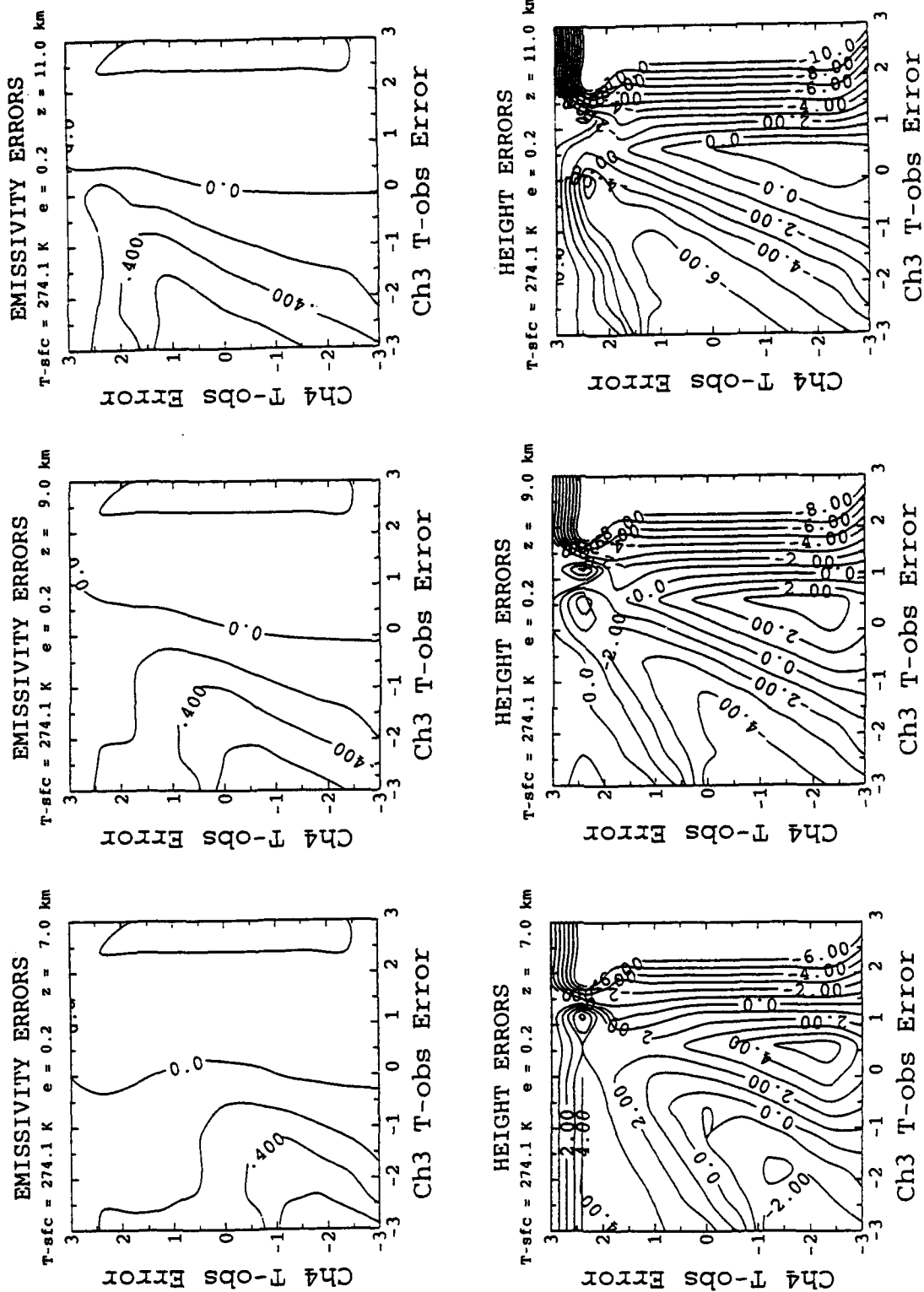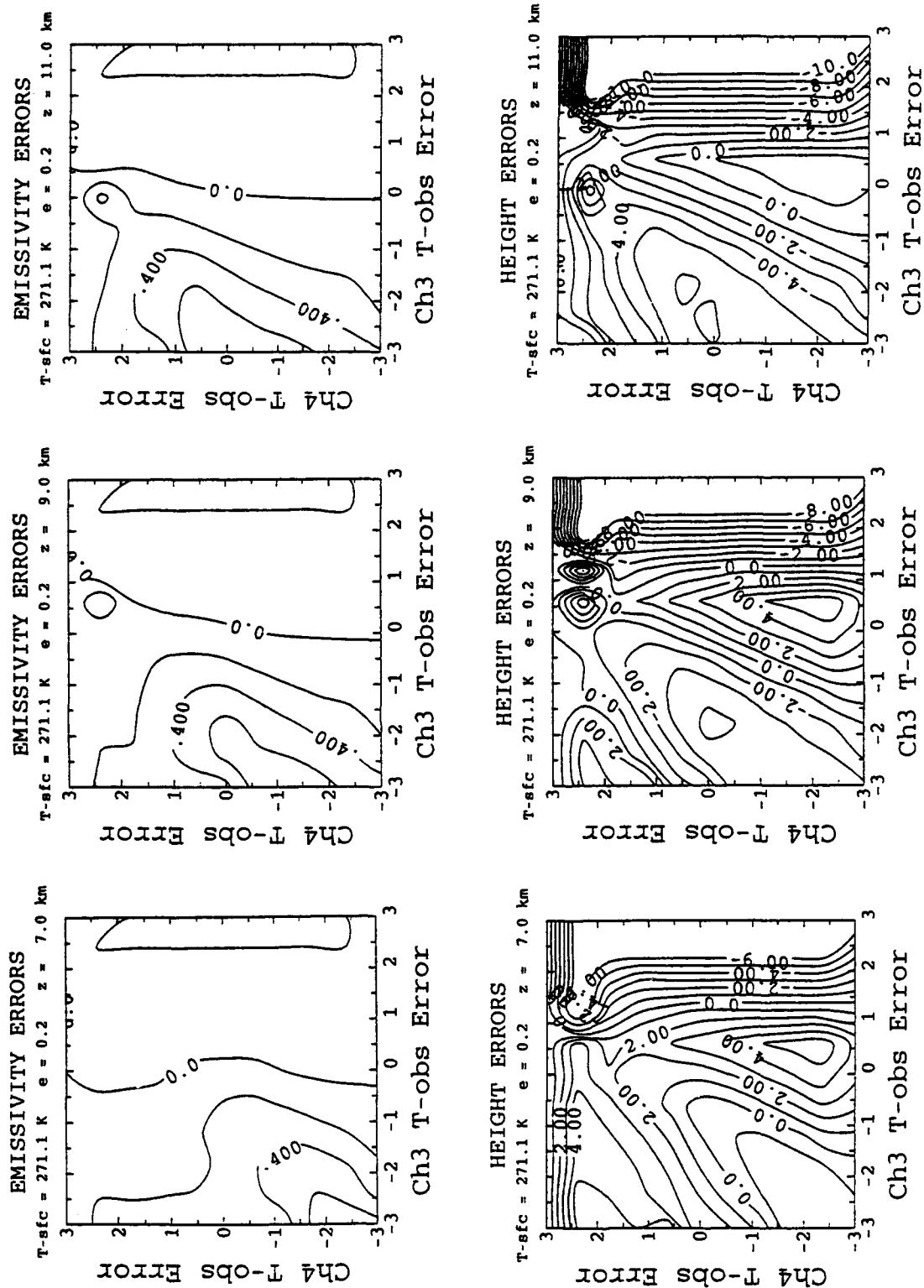
Figure 2. Plots of AIRC - Retrieved Cirrus Emissivity Errors (dimensionless) and Cloud Height Errors (km) as a Function of Brightness Temperature Measurement Errors ΔT_3 and ΔT_4. Error Plots are for T_{sfc} = 277.1 K (ΔT_{sfc} = +3 K) and True Cirrus Emissivity ε_4 = 0.2.
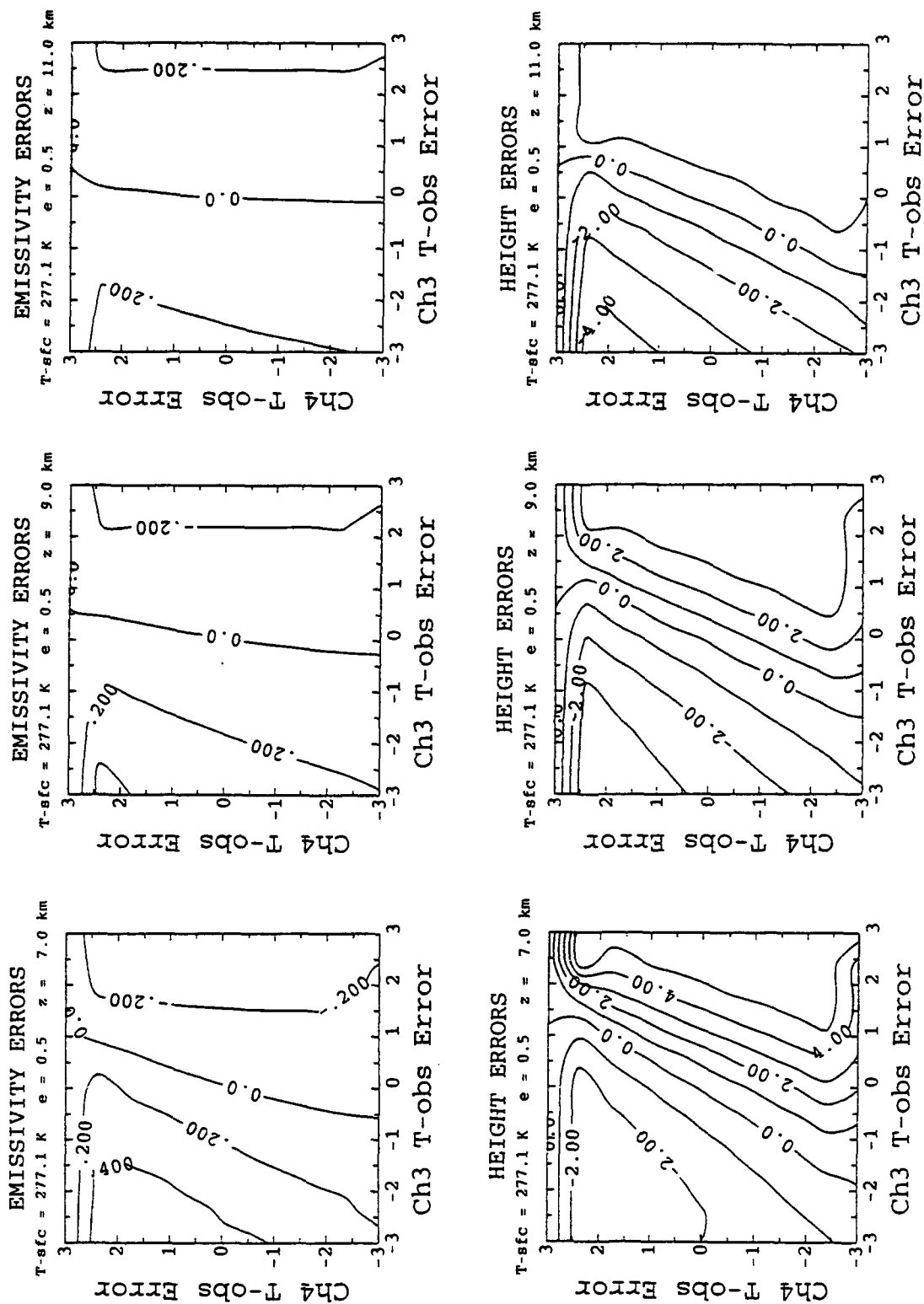
Figure 3. Plots of AIRC - Retrieved Cirrus Emissivity Errors (dimensionless) and Cloud Height Errors (km) as a Function of Brightness Temperature Measurement Errors ΔT_3 and ΔT_4. Error Plots are for $T_{sfc} = 274.1$ K ($\Delta T_{sfc} = 0$ K) and True Cirrus Emissivity $\varepsilon_4 = 0.2$.
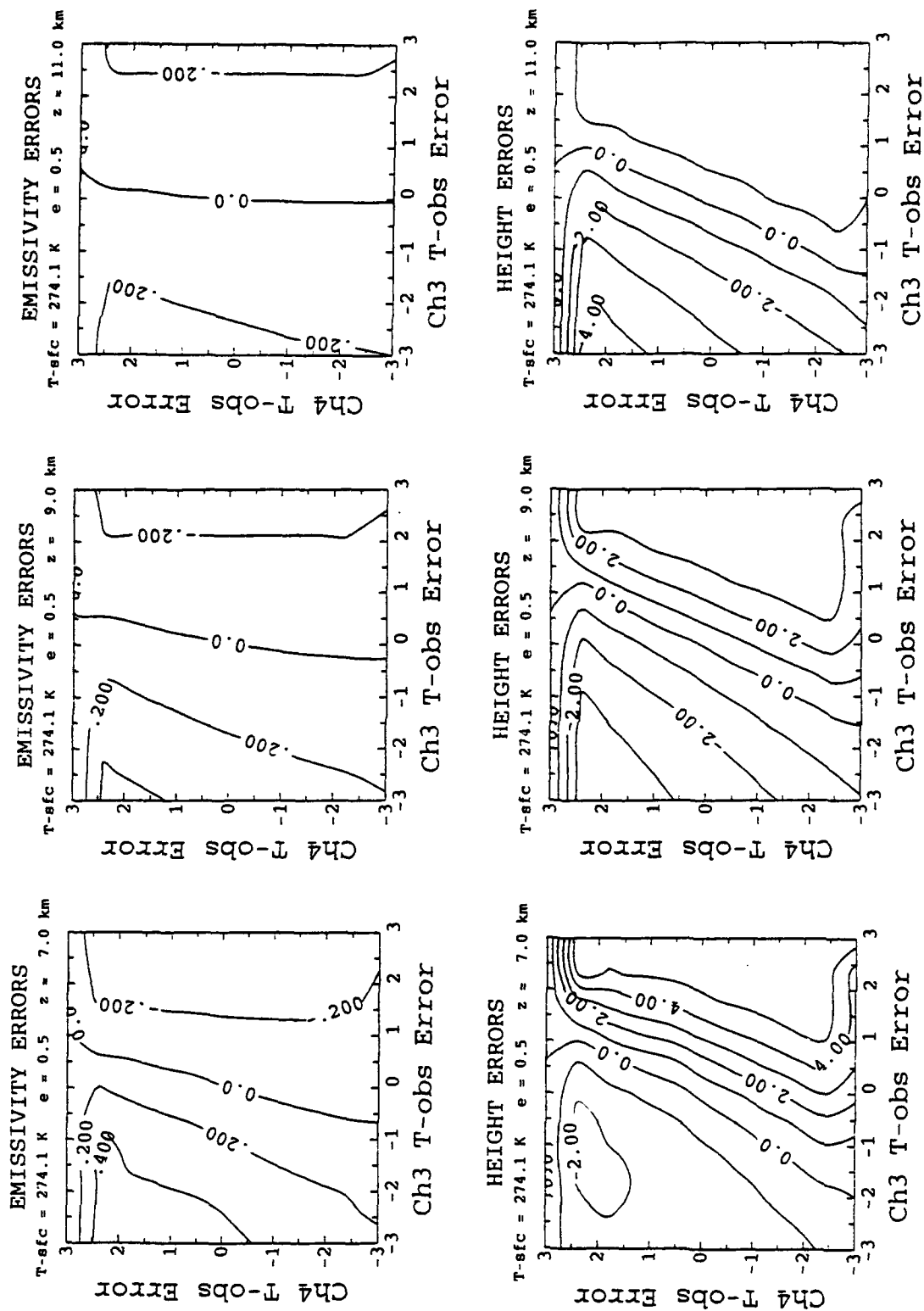
29

Figure 4. Plots of AIRC - Retrieved Cirrus Emissivity Errors (dimensionless) and Cloud Height Errors (km) as a Function of Brightness Temperature Measurement Errors ΔT_3 and ΔT_4. Error Plots are for T_{sfc} = 271.1 K (ΔT_{sfc} = -3 K) and True Cirrus Emissivity ε_4 = 0.2.

Figure 5. Plots of AIRC - Retrieved Cirrus Emissivity Errors (dimensionless) and Cloud Height Errors (km) as a Function of Brightness Temperature Measurement Errors ΔT_3 and ΔT_4. Error Plots are for $T_{sfc} = 277.1$ K ($\Delta T_{sfc} = +3$ K) and True Cirrus Emissivity $\varepsilon_4 = 0.5$.
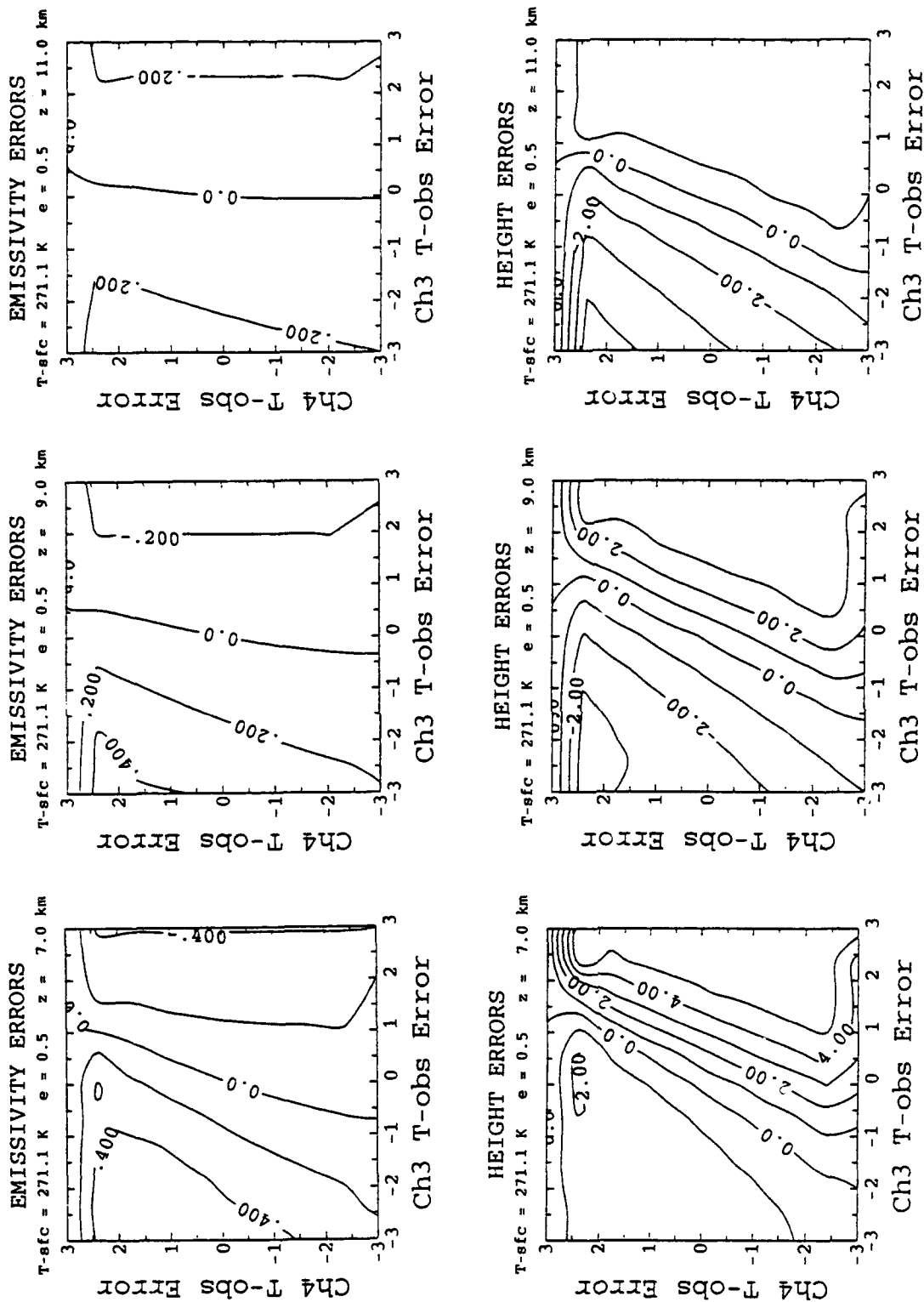
31

Figure 6. Plots of AIRC - Retrieved Cirrus Emissivity Errors (dimensionless) and Cloud Height Errors (km) as a Function of Brightness Temperature Measurement Errors ΔT_3 and ΔT_4. Error Plots are for $T_{sfc} = 274.1$ K ($\Delta T_{sfc} = 0$ K) and True Cirrus Emissivity $\epsilon_4 = 0.5$.
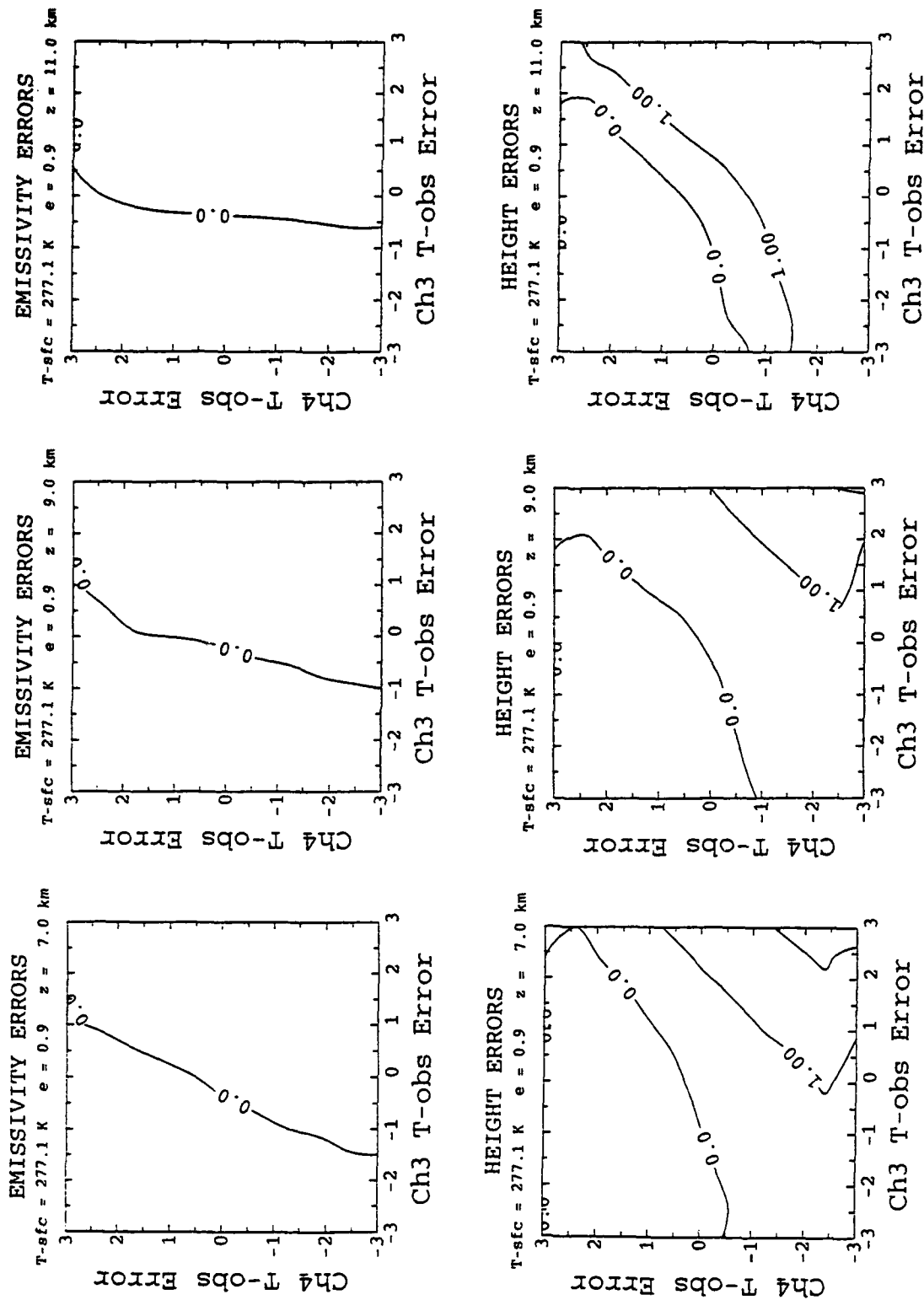
32

Figure 7. Plots of AIRC - Retrieved Cirrus Emissivity Errors (dimensionless) and Cloud Height Errors (km) as a Function of Brightness Temperature Measurement Errors ΔT_3 and ΔT_4. Error Plots are for $T_{sfc} = 271.1$ K ($\Delta T_{sfc} = -3$ K) and True Cirrus Emissivity $\varepsilon_4 = 0.5$.
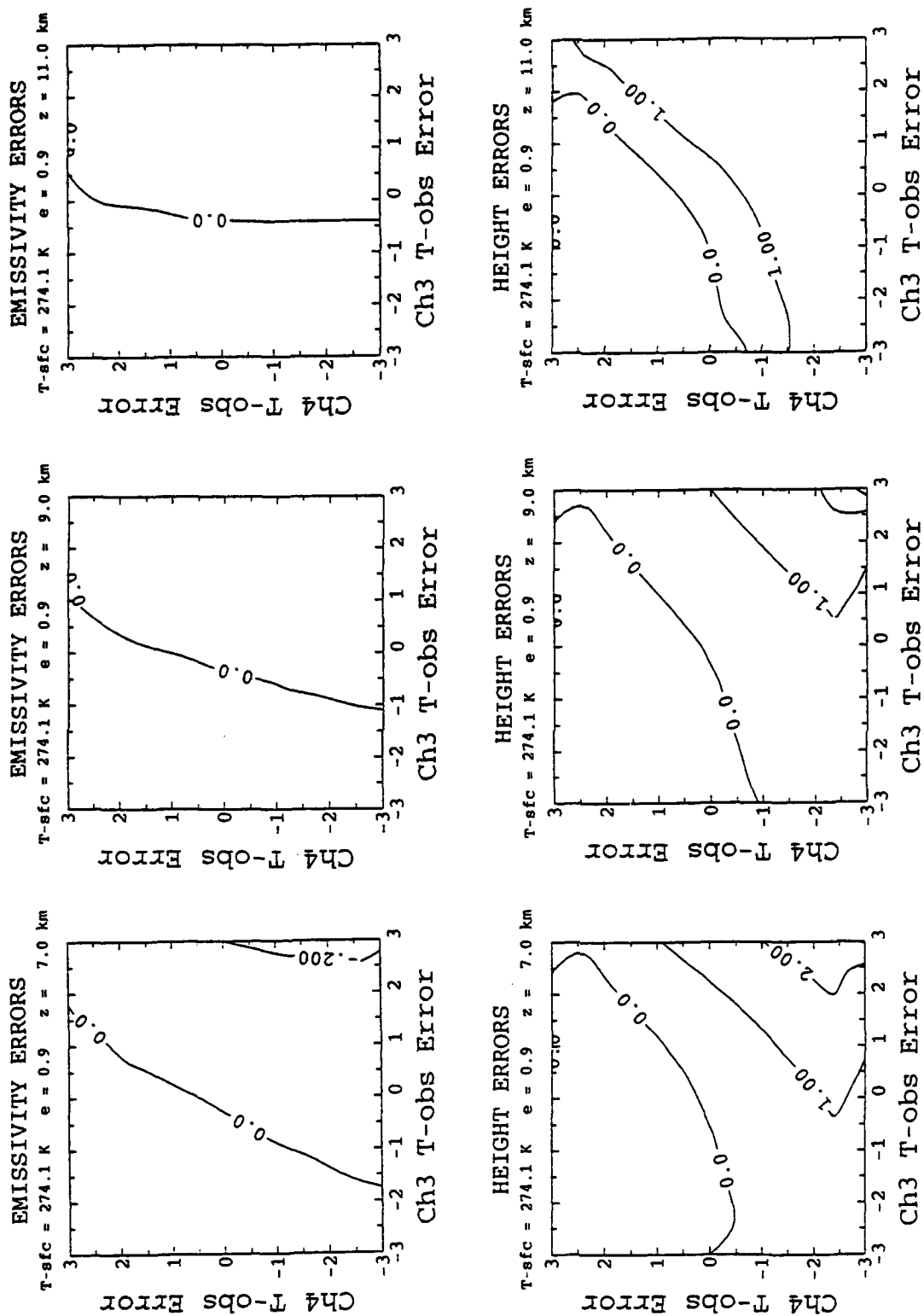
Figure 8. Plots of AIRC - Retrieved Cirrus Emissivity Errors (dimensionless) and Cloud Height Errors (km) as a Function of Brightness Temperature Measurement Errors ΔT_3 and ΔT_4. Error Plots are for T_{sfc} = 277.1 K (ΔT_{sfc} = +3 K) and True Cirrus Emissivity ε_4 = 0.9.

34

Figure 9. Plots of AIRC - Retrieved Cirrus Emissivity Errors (dimensionless) and Cloud Height Errors (km) as a Function of Brightness Temperature Measurement Errors ΔT_3 and ΔT_4. Error Plots are for $T_{sfc} = 274.1$ K ($\Delta T_{sfc} = 0$ K) and True Cirrus Emissivity $\varepsilon_4 = 0.9$.
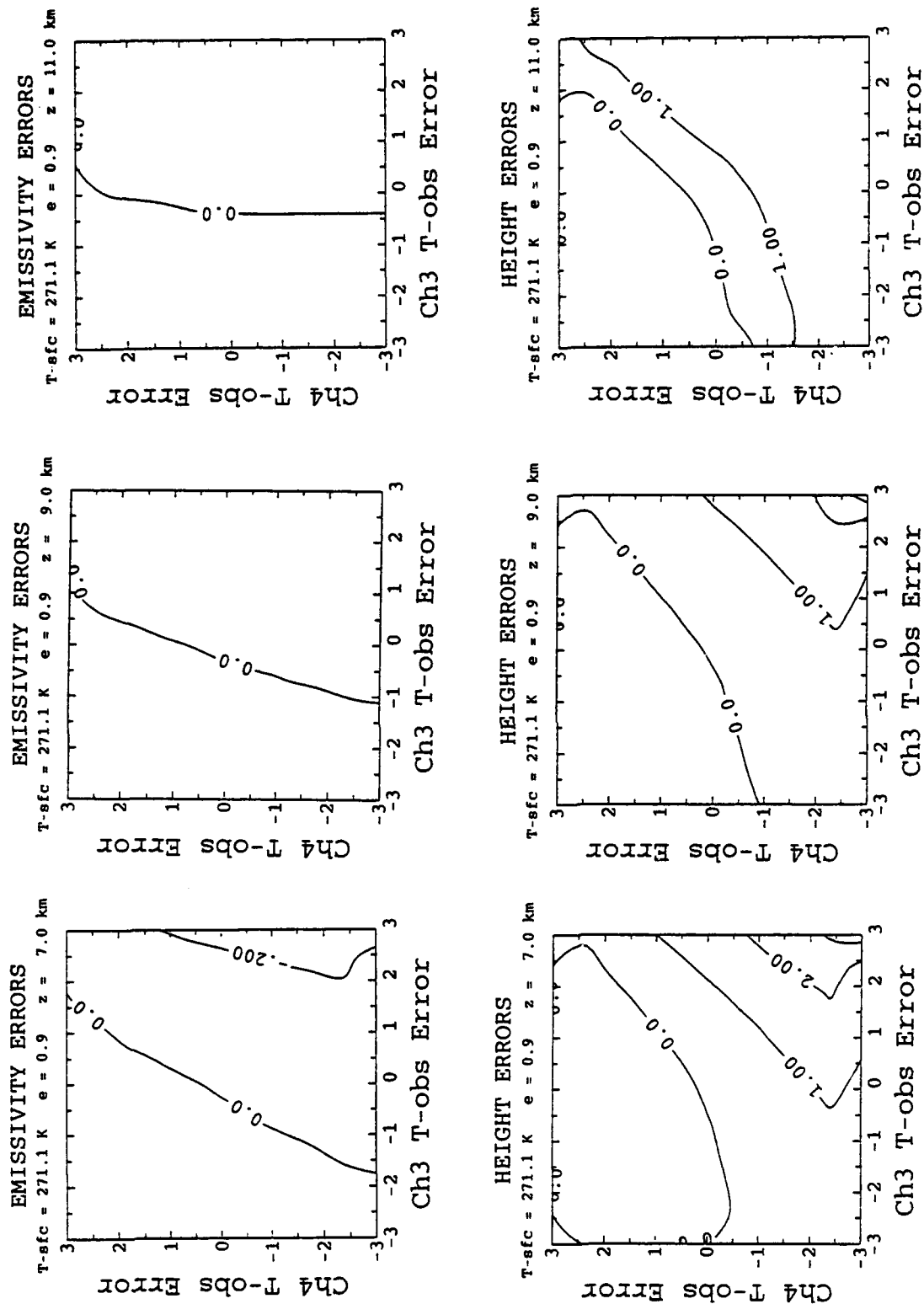
35

Figure 10. Plots of AIRC - Retrieved Cirrus Emissivity Errors (dimensionless) and Cloud Height Errors (km) as a Function of Brightness Temperature Measurement Errors ΔT_3 and ΔT_4. Error Plots are for $T_{sfc} = 271.1$ K ($\Delta T_{sfc} = -3$ K) and True Cirrus Emissivity $\varepsilon_4 = 0.9$.